THE JOURNAL OF BIOLOGICAL CHEMISTRY VOL. 287, NO. 6, pp. 4335–4347, February 3, 2012

Fucose-binding Lectin from Opportunistic Pathogen *Burkholderia ambifaria* Binds to Both Plant and Human Oligosaccharidic Epitopes*[S]

Received for publication, October 18, 2011, and in revised form, December 3, 2011 Published, JBC Papers in Press, December 14, 2011, DOI 10.1074/jbc.M111.314831

Aymeric Audfray[‡], Julie Claudinon[§], Saïda Abounit[¶], Nathalie Ruvoën-Clouet[‖], Göran Larson[**], David F. Smith[‡‡], Michaela Wimmerová[§§], Jacques Le Pendu[‖], Winfried Römer[§¶], Annabelle Varrot[‡], and Anne Imberty[‡1]

*From the [‡]Centre de Recherche sur les Macromolécules Végétales (CERMAV)-CNRS, Université Joseph Fourier and Institut de Chimie Moléculaire de Grenoble, 38041 Grenoble, France, the [§]Institute of Biology II and Center for Biological Signaling Studies (BIOSS), Albert Ludwigs University Freiburg, 79104 Freiburg, Germany, the [¶]Traffic, Signaling, and Delivery Group, Centre de Recherche, CNRS UMR 144, Institut Curie, 75248 Paris, France, [‖]INSERM U892, Institut de Recherche Thérapeutic (IRT-UN), University of Nantes, 44007 Nantes, France, the **Department of Clinical Chemistry and Transfusion Medicine, Sahlgrenska University Hospital, 41345 Gothenburg, Sweden, the [‡‡]Department of Biochemistry, Emory University School of Medicine, Atlanta, Georgia 30322, and the [§§]Central European Institute of Technology, Masaryk University, 62500 Brno, Czech Republic*

Background: *Burkholderia ambifaria* is a plant-associated bacteria responsible for opportunistic infections in human.
Results: The β-propeller BambL lectin is specific for fucosylated oligosaccharides with higher affinity for biological samples from secretor individuals.
Conclusion: The recombinant BambL lectin binds to both plant and human oligosaccharides.
Significance: The diversity of fucosylated epitopes may play a role in host recognition in mammals and plants.

***Burkholderia ambifaria* is generally associated with the rhizosphere of plants where it has biocontrol effects on other microorganisms. It is also a member of the *Burkholderia cepacia* complex, a group of closely related bacteria that cause lung infections in immunocompromised patients as well as in patients with granulomatous disease or cystic fibrosis. Our previous work indicated that fucose on human epithelia is a frequent target for lectins and adhesins of lung pathogens (Sulák, O., Cioci, G., Lameignère, E., Balloy, V., Round, A., Gutsche, I., Malinovská, L., Chignard, M., Kosma, P., Aubert, D. F., Marolda, C. L., Valvano, M. A., Wimmerová, M., and Imberty, A. (2011) *PLoS Pathog.* 7, e1002238). Analysis of the *B. ambifaria* genome identified BambL as a putative fucose-binding lectin. The 87-amino acid protein was produced recombinantly and demonstrated to bind to fucosylated oligosaccharides with a preference for αFuc1–2Gal epitopes. Crystal structures revealed that it associates as a trimer with two fucose-binding sites per monomer. The overall fold is a six-bladed β-propeller formed by oligomerization as in the *Ralstonia solanacearum* lectin and not by sequential domains like the fungal fucose lectin from *Aleuria aurantia*. The affinity of BambL for small fucosylated glycans is very high as demonstrated by microcalorimetry (K_D < 1 μM). Plant cell wall oligosaccharides and human histo-blood group oligosaccharides H-type 2 and Lewis Y are bound with equivalent efficiency. Binding to artificial glycosphingolipid-containing vesicles, human saliva, and lung tissues confirmed that BambL could recognize a wide spectrum of fucosylated epitopes, albeit with a lower affinity for biological material from nonsecretor individuals.**

The *Burkholderia cepacia* complex (Bcc)[2] is a group of genetically distinct but phenotypically similar Gram-negative bacteria that is divided into at least 17 species (1, 2). Bcc species have interesting antifungal properties that give them environmental and biotechnological potential (3). Usually nonpathogenic for healthy individuals, Bcc can cause a variety of infections in immunocompromised patients, as well as in patients with cystic fibrosis (CF) and granulomatous disease. It is responsible for the "cepacia syndrome" that leads to rapid lung deterioration and death in most cases (4, 5). A number of virulence factors have been described and characterized in Bcc isolates, including pili, flagella, the type III secretion system, surface exopolysaccharides, proteases, and other secreted enzymes (6). Unfortunately, most of the Bcc organisms are highly resistant to all major classes of antibiotics (7) and are able to form biofilms, which makes the treatment of patients infected with Bcc problematic.

* This work was supported by CNRS-INSERM, the German Excellence Initiative of the Deutsche Forschungsgemeinschaft, and the Association Vaincre la Mucoviscidose. This work was also supported by Agence Nationale de la Recherche Grants NeoLect 11-BSV5-002-01 (to A. I., W. R., and J. L. P.) and GlycanClust (to W. R.) and by grants from the Czech Science Foundation (GA303/09/1168) and the CEITEC-Central European Institute of Technology (CZ.1.05/1.1.00/02.0068) from the European Regional Development Fund (to M. W.).

[S] This article contains supplemental Figs. S1–S4 and Tables S1–S3.

The atomic coordinates and structure factors (codes 3ZW0, 3ZWE, 3ZW2, and 3ZZV) have been deposited in the Protein Data Bank, Research Collaboratory for Structural Bioinformatics, Rutgers University, New Brunswick, NJ (http://www.rcsb.org/).

[1] To whom correspondence should be addressed: CERMAV-CNRS, 601 Rue de la Chimie, BP53, 38041 Grenoble Cedex 9, France. Tel.: 33-476037636; Fax: 33-476547203; E-mail: Imberty@cermav.cnrs.fr.

[2] The abbreviations used are: Bcc, *Burkholderia cepacia* complex; CF, cystic fibrosis; SPR, surface plasmon resonance; ITC, isothermal titration calorimetry; Bicine, *N*,*N*-bis(2-hydroxyethyl)glycine; BambL, fucose-binding lectin from *Burkholderia ambifaria*; RSL, *Ralstonia solanacearum* lectin; DOPC, 1,2-dioleoyl-*sn*-glycero-3-phosphocholine; HPC, hexadecanoyl phosphatidylcholine; GUV, giant unilamellar vesicle.

Genomovar VII of Bcc, also called *Burkholderia ambifaria*, is an example of an organism with dual action, as it is able to protect plants against fungal infection but also to cause infections in human (4, 8). *B. ambifaria* is a major component of the rhizosphere of many crop plants including maize (9). It has been used commercially as a biopesticide for a few years (10). At the same time, this species is also an opportunistic human pathogen, particularly problematic in CF patients (8). No clear distinction can be established between environmental and pathogenic *B. ambifaria* isolates, and their adaptation to different environment seems to be related to phase variation (11).

Opportunistic bacteria often use lectins, *i.e.* protein receptors with high specificity for glycoconjugates, to recognize and adhere to human tissues (12, 13). More particularly, fucosylated glycoconjugates are present in higher quantity in CF lungs (14) and appear to be a target for lectins from pathogenic bacteria such as *Pseudomonas aeruginosa* (15) and *Burkholderia cenocepacia* (16, 17). Fucosylated glycans are also present in plant cell walls and can act as targets for bacterial receptors (18).

Analysis of the available genomes of *B. ambifaria* allowed us to identify a new fucose-binding lectin, BambL, with no similarities to lectins from *P. aeruginosa* and *B. cenocepacia* but related to lectins from the fungus *Aleuria aurantia* and from the phytopathogenic bacterium *Ralstonia solanacearum* (18). The present article describes the cloning, production, and binding properties of recombinant BambL. Based on its specificity as determined by screening of a glycan microarray, a large panel of fucosylated oligosaccharides (Table 1) was screened by glycan array and SPR and rationalized through the crystal structures of several complexes. The very strong affinity for human epitopes H-type 2 and Lewis Y and for plant cell wall fucosylated xyloglucans was confirmed by titration microcalorimetry. Binding to membrane-embedded glycosphingolipids was tested on a giant unilamellar vesicle model. Possible involvement in binding to human tissue was evaluated by binding to saliva and airway epithelia from humans with different blood group phenotypes.

TABLE 1
Name and structures of fucosylated oligosaccharide epitopes studied

name	abbreviation(s)	structure
Core N-glycan fucose	Fuc6GlcNAc	Fucα1-6GlcNAc
Blood group H disaccharide	H-di	Fucα1-2Gal
H-type 1 tetrasaccharide	H-type 1	Fucα1-2Galβ1-3GlcNAcβ1-3Gal
H-type 2 tetrasaccharide	H-type 2	Fucα1-2Galβ1-4GlcNAcβ1-3Gal
H-type 5 trisaccharide	H-type 5 / FucLac	Fucα1-2Galβ1-4Glc
Blood group A trisaccharide	A-tri	GalNAcα1-3Gal /2 Fucα1
A type 2 pentasaccharide	A-penta	GalNAcα1-3Galβ1-4GlcNAcβ1-3Gal /2 Fucα1
B type 2 pentasaccharide	B-penta	Galα1-3Galβ1-4GlcNAcβ1-3Gal /2 Fucα1
B type 5 tetra	B-tetra	Galα1-3Galβ1-4Glc /2 Fucα1
Lewis X tetrasaccharide	Le^X	Galβ1-4GlcNAcβ1-3Gal /3 Fucα1
Lewis Y pentasaccharide	Le^Y	Galβ1-4GlcNAcβ1-3Gal /2 /3 Fucα1 Fucα1
Lewis a tetrasaccharide	Le^a	Galβ1-3GlcNAcβ1-3Gal /4 Fucα1
Lewis b pentasaccharide	Le^b	Galβ1-3GlcNAcβ1-3Gal /2 /4 Fucα1 Fucα1
XFG xyloglucan heptasaccharide	XFG	Galβ1-2Xylα1-6Glcβ1-4Glc /2 /4 Fucα1 Xylα1-6Glcβ1

EXPERIMENTAL PROCEDURES

Materials—α-Methyl-fucoside was purchased from Sigma-Aldrich and disaccharides (Fucα1–2Gal, Fucα1–6GlcNAc, and lactose) and fucosyllactose (Fucα1–2Galβ1–4Glc) from Dextra (Reading, United Kingdom). All other human histo-blood group oligosaccharides and xyloglucan were purchased from Elicityl (Crolles, France).

Production of Recombinant Bacterial Lectins—A nucleotide sequence coding for the peptide sequence of BambL from *B. ambifaria* AMMD (GenBank™ accession number YP_777296 or UniProt ID Q0B4G1_BURCM) was synthesized after codon optimization for expression in *Escherichia coli* (GenScript, Piscataway, NJ). It was introduced into the expression vector pET25b using NdeI and BamHI restriction sites. The pET25-BambL vector was transformed into *E. coli* BL21(DE3) (Novagen), and cells harboring pET25-BambL plasmid were grown in LB broth containing 100 μg ml^{-1} ampicillin at 37 °C until A_{600} reached 0.7. The cells were then cultured for 16 h after the addition of 0.5 mM isopropyl-β-D-thiogalactopyranoside. After centrifugation (7000 × *g* for 15 min), bacteria were resuspended in equilibration buffer (20 mM Tris/HCl, pH 7.5, 150 mM NaCl) and broken by cell disruption at a pressure of 1.7 kilobars (constant cell disruption system). After centrifugation (50000 × *g*, 30 min at 4 °C) and filtration, affinity chromatography on a mannose-agarose column (Sigma-Aldrich) was performed on the supernatant. BambL was allowed to bind to immobilized mannose in equilibration buffer, and after washing (20 mM Tris/HCl pH 7.5, 1 M NaCl) it was eluted with 100 mM mannose in equilibration buffer. Purified protein was dialyzed extensively against ultrapure water for 7 days, freeze-dried, and stored at 4 °C. Recombinant RSL was produced as described earlier (18).

Glycan Array—Purified BambL and RSL samples were labeled with Alexa Fluor 488 (Invitrogen) according to the manufacturer's instructions and repurified on a D-Salt polyacrylamide desalting column (Pierce). Alexa-labeled proteins were used for glycan array screening with the standard procedure of the Protein-Glycan Interaction Core (H) of the Consortium for Functional Glycomics.

To determine the fine specificity of BambL, its binding to glycans on version 4.1 of the CFG glycan array comprising 465 natural and synthetic glycans was analyzed in a dose-dependent

manner as described previously (19) at 1, 0.2 and 0.05 μg ml^{-1} of lectin, dissolved in 20 mM HEPES, 140 mM NaCl, and 5 mM $CaCl_2$, pH 7.5. Briefly, the binding of BambL, at different concentrations, to each glycan was normalized to percentages of the highest relative fluorescence unit value for each analysis, and the percent maximum binding for each glycan at the different lectin concentrations was averaged to obtain an average ranking. The data were sorted according to the average ranking to obtain the order of relative binding of the glycans on the array.

Microcalorimetry—Recombinant lyophilized BambL was dissolved in buffer (20 mM Tris/HCl, pH 7.5, NaCl 150 mM) and degassed. The protein concentration was checked by measuring A_{280} by using a theoretical molar extinction coefficient of 40,450 M^{-1} cm^{-1}. Carbohydrate ligands were dissolved in the same buffer, degassed, and loaded in the injection syringe. ITC was performed with a VP-ITC microcalorimeter (MicroCal Inc.). The BambL solution was placed in a 1.4478-ml sample cell at 25 °C. Titration was performed with 10-μl injections of carbohydrate ligands every 300 s. Data were fitted with MicroCal Origin 7 software according to standard procedures. The fitted data yielded the stoichiometry (n), association constant (K_a), and enthalpy of binding (ΔH). Other thermodynamic parameters (*i.e.* changes in free energy (ΔG) and entropy (ΔS)) were calculated from the equation $\Delta G = \Delta H - T\Delta S = RT\ln K_a$, in which T is the absolute temperature and $R = 8.314$ J mol^{-1} K^{-1}. Two independent titrations were performed for each ligand tested.

Surface Plasmon Resonance—SPR inhibition experiments were performed on a Biacore X100 instrument (GE Healthcare) at 25 °C in HBS buffer (10 mM Hepes/NaOH, pH 7.5, 150 mM NaCl, 0.05% Tween 20) at a flow rate of 10 μl min^{-1}. Streptavidin was immobilized on a research grade CM5 chip using standard procedures, and 300 resonance units of biotinylated polyacrylamide probes (Lectinity, 200 μg ml^{-1}) bearing galactose or fucose were captured on channels 1 (reference) and 2, respectively. Inhibition experiments were performed with the fucosylated channel 2, and plots represent the subtracted data (channel 2 − channel 1). Inhibition studies consisted of the injection (association 240 s, dissociation 600 s) of incubated (>30 min at room temperature) mixtures of BambL (1 μM) and various concentrations of inhibitor (3-fold cascade dilutions). For each inhibition assay, BambL was injected to observe the full adhesion of the lectin onto the sugar-coated surface (0% inhibition). The chip was fully regenerated by two successive injections of L-fucose (120 s, 1 M in running buffer).

Binding was measured as resonance units over time after blank subtraction, and data were then evaluated by using the Biacore X100 evaluation software, version 2.0. For IC_{50} evaluation, the response was considered as the amount of lectin bound to the sugar surface at equilibrium in the presence of a defined concentration of inhibitor. Inhibition curves were obtained by plotting the percentage of inhibition against the inhibitor concentration (logarithmic scale).

Protein Crystallography—Crystals of BambL complexed with fucosylated oligosaccharides were obtained by the hanging drop vapor diffusion method using 2 μl of drops containing a 50:50 (v/v) mix of protein and reservoir solution at 20 °C. Lyophilized protein was dissolved in Tris/HCl buffer, pH 7.5, and NaCl 150 mM at 1 mM and incubated for 1 h with H-type 5 (FucLac), H-type 1, H-type 2, and B-tetra oligosaccharides (5 mM) at room temperature prior to co-crystallization. Crystals of the different complexes were obtained from 200 mM trisodium citrate, 100 mM sodium acetate, pH 5.0, and 24% PEG 8000 for the complex with FucLac; with 3 M malonate, pH 6.0, for H-type 1 and H-type 2 complexes; and with 1 M lithium chloride, 100 mM Bicine, pH 9.0, and 30% PEG 6000 for the B-tetra complex. For all crystals except the one with B-tetra, 10% ethylene glycol was added to the mother liquor prior to mounting in a cryoloop and freezing in liquid nitrogen. Diffraction data were collected at 100 K at the European Synchrotron Radiation Facility (Grenoble, France) at station ID14-EH4 or BM30A using an ADSC Q4 CCD detector. The data were processed using MOSFLM (20) and scaled and converted to structure factors using SCALA. All further computing was performed using the CCP4 suite (21) unless otherwise stated. Data quality statistics are summarized in Table 2.

The molecular replacement technique was used to solve the different structures with PHASER (22) and the coordinates of the *Ralstonia solanacearum* lectin (RSL) (Protein Data Bank code 2BT9) were used as the search model (18) for the FucLac complex structure. For the other liganded structures, the latest coordinates (Protein Data Bank code 3ZW0) were used as the search model. Five percent of the observations were set aside for cross-validation analysis (23), and hydrogen atoms were added in their riding positions and used for geometry and structure-factor calculations. The structure was refined by restrained maximum likelihood refinement using REFMAC (24) iterated with manual rebuilding in Coot (25). In each complex, incorporation of the ligands was performed after inspection of the mF_o − DF_c weighted maps. The initial maps revealed clear density for the fucose moiety, and the number of additional sugars that could be observed depended on the sites and ligand. Water molecules, introduced automatically using Coot, were inspected manually. The stereochemical quality of the models was assessed with the program ProCheck (26), and coordinates were deposited in the Protein Data Bank under codes 3ZW2 (H-type 1), 3ZWE (B-tetra), and 3ZZV (H-type 2). Molecular drawings were prepared using the PyMOL molecular graphics system (DeLano Scientific, Palo Alto, CA) and LIGPLOT (27).

Production of Giant Unilamellar Vesicles by Electroformation and Lectin Binding to Glycosphingolipid-containing Liposomes—The lipids 1,2-dioleoyl-*sn*-glycero-3-phosphocholine (DOPC) and cholesterol were purchased from Avanti Polar Lipids. BODIPY-FL-C5 hexadecanoyl phosphatidylcholine (HPC) was from Molecular Probes (Invitrogen) and globotriaosylceramide from Matreya LLC. The fucosylated type 1 chain glycosphingolipids and the precursor lactotetraosylceramide were isolated from meconia, pooled according to blood group ABO, and characterized in detail as described previously for a human O Le(a−b+) secretor (28).

Giant unilamellar vesicles (GUVs) were composed of DOPC (spiked with 1 mol % BODIPY-FL-C5-HPC, green), cholesterol (30 mol %), and various glycosphingolipid species (5 mol %). GUVs were grown at room temperature using the electrofor-

TABLE 2

Data collection and refinement statistics of BambL complexed with different glycans

r.m.s.d., root mean square deviation; DPI, Cruickshank's dispersion precision indicator; PDB, Protein Data Bank.

Data collection				
Ligand	FucLac	B-tetra	H-type 1	H-type 2
Beamline	BM30 A	BM30 A	ID14 EH4	ID14-1
Wavelength (Å)	0.9797	0.9797	1.1399	0.933
Space group	$P2_12_12_1$	$P2_12_12_1$	$P2_1$	$P2_1$
Cell dimensions				
a, *b*, *c* (Å)	45.11, 47.25, 98.33	47.98, 49.14, 102.71	34.64, 47.57, 72.94	35.74, 47.7, 74.60
α, β, γ (°)	90, 90.0, 90	90, 90, 90	90, 103.2, 90	90, 100.8, 90
Resolution (outer shell) (Å)	49.16-1.60 (1.69-1.60)	44.33-1.75 (1.84-1.75)	39.42-1.60 (1.69-1.60)	29.07-1.68 (1.77-1.68)
Measured/Unique reflections	255,601/2,6647	152,409/24,165	81,127/2,9207	21,2606/27,476
Average multiplicity (outer shell)	3.7 (2.6)	3.3 (2.4)	2.8 (2.5)	3.5 (2.8)
R_{merge} (outer shell)	0.031 (0.055)	0.053 (0.354)	0.068 (0.183)	0.038 (0.387)
Completeness (%) (outer shell)	93.7 (70.5)	96.0 (79.9)	95.3 (78.9)	96.9 (81.2)
Average $I/\sigma I$ (outer shell)	16.6 (13.2)	9 (2.1)	7.1 (2.5)	11.3 (1.9)
Wilson B	10.2	21.3	17.2	21.3
Refinement				
R_{cryst}/R_{free}	14.3/18.8	20.8/26.6	16.0/20.2	21.1/27.1
r.m.s.d. bonds (Å)	0.015	0.016	0.015	0.016
r.m.s.d. angles (°)	1.537	1.623	1.681	1.875
r.m.s.d. chiral (Å^3)	0.096	0.110	0.105	0.122
Protein atoms[a]	676/692/669	661/664/669	667/675/673	665/661/667
Bfac (Å^2)	8.9/8.1/9.2	28.5/25.9/19.2	17.8/18.4/15.4	19.1/26.6/27.5
Water molecules[a]	153/132/114	68/68/81	95/89/76	106/58/44
Bfac (Å^2)	19.3/ 17.5/19.7	30.3/31.7/30.1	29.0/30.9/29.3	29.3/ 31.8/32.0
Ligand atoms[a]	11	33/55/55	58/72/86	72/47/72
Bfac (Å^2)	11.3	30.8/30.4/21.2	21.5/26.8/19.7	26.9/34.3/34.2
DPI (Å)	0.094	0.148	0.096	0.136
PDB code	3ZW0	3ZWE	3ZW2	3ZZV

[a] For chains A/B/C.

mation technique on indium-tin oxide (ITO)-coated slides essentially as described previously (29, 30). Briefly, lipid mixtures were dissolved in chloroform at a final concentration of 0.5 mg ml^{-1}, and 15 μl of solution was spread on the conductive faces of ITO slides. After at least 2 h of drying under vacuum, GUVs were grown in a 290 mosM sucrose solution by applying an alternating electric field from 20 mV to 1.1 V for 3 h. Under all conditions, BambL (10 μg ml^{-1}) was incubated with GUVs at room temperature and examined under an inverted confocal fluorescence microscopes (LSM 510, Carl Zeiss, and A1R, Nikon) equipped with oil immersion objectives.

Binding to Human Saliva and Tissues—Saliva samples collected from 59 healthy individuals of known ABO, secretor, and Lewis phenotypes, with confirmed *FUT2* (secretor) and *FUT3* (Lewis) genotypes (31, 32), were selected to cover the ABO, secretor, and Lewis phenotypic diversity. The study was approved by the Nantes University Hospital Review Board (study BRD02/2-P), and informed consent was obtained from all saliva donors. After collection, samples were boiled for 10 min and centrifuged for 5 min at 13,000 × *g*. To assay BambL binding to saliva, MaxiSorb plates (Thermo Fisher Scientific) were coated in duplicates with saliva samples diluted 1/1000 in 100 mM carbonate buffer, pH 9.6. After blocking with 5% defatted dried cow's milk in PBS for 1 h, biotinylated BambL at 0.1 μg ml^{-1}, or biotinylated UEA-I (Sigma-Aldrich) used as a control at 1 μg ml^{-1} in PBS 5% defatted dried cow's milk, was added. After samples were incubated for 2 h at 37 °C, HRP-conjugated avidin (Vector Laboratories, Burlingame, CA) diluted 1/3000 in PBS 5% defatted dried cow's milk was added and incubated for 1 h at 37 °C. Between each step, plates were washed three times with PBS, 5% Tween 20. The enzyme signals were detected using 3,3′,5,5′-tetramethylbenzidine (TMB) as substrate (BD Biosciences) and then read at 450 nm. Inhibition by free sugars was performed by preincubating BambL at 1 mg ml^{-1} with either 100 mM fucose or 5 mM 2′-fucosyllactose (Fucα2Galβ4Glc) for 2 h at room temperature prior to incubation on saliva samples as described above.

Human trachea, lung, and gastroduodenal junction samples (obtained from organ donors prior to passage of Law 88-1138 of December 20, 1988 (France), concerning resection of human tissues after death for scientific investigations) were used to prepare tissue microarrays. Tissues from 18 individuals were used: O secretor Lewis + (n = 8), A secretor Lewis+ (n = 3), B secretor Lewis+ (n = 2), O secretor Lewis− (n = 1), and O nonsecretor Lewis+ (n = 4). Sections were deparafinated through bathing in LMR®SOL (Labomoderne) and ethanol. Endogenous peroxidase activity was blocked with 0.3% hydrogen peroxide. Nonspecific binding was blocked with 1% BSA in PBS for 30 min. After washing with PBS, biotinylated BambL diluted at 0.1 μg ml^{-1} in 0.1% BSA/PBS was incubated overnight at 4 °C. Following three washes with PBS, HRP-conjugated avidin (Vector Laboratories) diluted 1/2000 in 0.1% BSA/PBS was added and the mixture was incubated for 45 min at room temperature. After three more washings with PBS, substrate was added to the slides (AEC kit, Vector Laboratories) followed by Mayer's hemalum solution (Merck) for contrast staining.

RESULTS

Production and Characterization of BambL—The BambL gene has been identified by sequence homology (76.5% protein sequence identity) with RSL (18) in chromosome 2 of the *B. ambifaria* AMMD genome. Except for those two species, this gene has not been identified in other bacterial genomes. BambL has been produced recombinantly in *E. coli* and purified in one step on a mannose-agarose column with a final yield of 5 mg liter^{-1} of culture. The strong hemagglutination activity (0.4

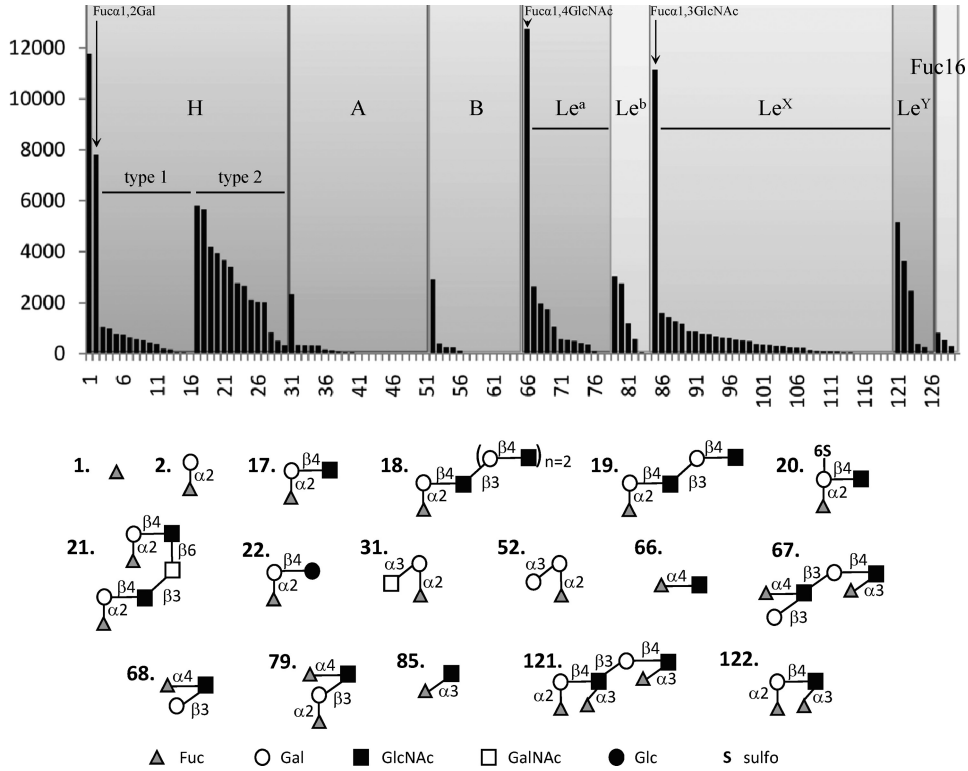

FIGURE 1. **Glycan array data for BambL (0.2 μg ml^{-1}) labeled with Alexa Fluor 488.** Only fucosylated epitopes have been selected for the display. The highest affinity ligand are represented schematically. Complete data for the 126 fucosylated oligosaccharides are given in supplemental Table S2. Complete data on the 465 glycans of the Consortium for Functional Glycomics glycan Array v4.1 are available on request.

μM hemagglutination units) can be inhibited by L-fucose (data not shown), suggesting that BambL is a fucose-binding lectin.

Carbohydrate Specificity of BambL—To determine its detailed specificity, BambL binding to the glycans on version 4.1 of the Consortium for Functional Glycomics glycan microarray were ranked according to their relative binding as shown in supplemental Table S1. Of the 465 glycans on v4.1 of the array, 129 contained fucose, and all 68 glycan structures with average rankings of >5% possessed a nonreducing terminal fucose residue. A more detailed analysis was performed by focusing only on the 129 fucosylated oligosaccharide (Fig. 1 and supplemental Table S2). BambL displays a preference on the glycan array for short glycans such as αFuc(1) and fucose disaccharides Fucα1–2Gal(2), Fucα1–3GlcNAc(85), and Fucα1–4GlcNAc(66), which had average ranking from 64 to 96% (supplemental Table S1). When looking at the larger fucosylated oligosaccharides that are present in human tissues, BambL has a clear preference for type 2 oligosaccharides containing the Fucα1–2Galβ1–4GlcNAc motif over the corresponding type 1 oligosaccharides. Strong binding is observed toward H-type 2 (blood group O) epitopes (epitopes 17–26, ranked at 14 to 46%). Substitution by a second fucose on GlcNAc is tolerated because Lewis Y (Le^Y) epitopes 121–123 (ranked at 29 to 45%) are also good ligands. On the other hand, H-type 1 epitopes 3–15 are only weakly recognized (ranked at 0 to 10%), and blood groups A and B are bound only as trisaccharides. Lewis a (ranked at 16 to 19%), Lewis X (at 14 to 26%), and Lewis b epitopes (containing terminal type 1 H, ranked at 32%) are medium range binding ligands. Likewise, Fucα1-6GlcNAc-containing *N*-glycans give only low signals. Such preference for short and linear glycans is unusual and points toward a deep binding site that can accommodate only a limited number of conformations for the fucose-terminated oligosaccharides. The related lectin RSL from *R. solanacearum* gave a very similar specificity profile when assayed on the glycan chips under the same conditions (supplemental Fig. S1).

TABLE 3

IC$_{50}$ of selected carbohydrates toward the binding of BambL to polyacrylamide-fuc determined by SPR

Inhibitor	IC$_{50}$	Inhibitory potential[a]
	μM	
A-tri	5.8	3.4
H-type 5/FucLac	6.5	3.1
H-di	8.2	2.4
Fuc6GlcNAc	8.3	2.4
αMeFuc	20	1
H-type2	24.4	0.82
Le^Y	65.3	0.31
Le^b	190	0.11
Le^a	280	0.07
H-type1	351	0.06
Le^X	429	0.05
A-penta	447	0.04
B-penta	501	0.04
Lactose	None	None

[a] Inhibitory potential is calculated relative to αMeFuc.

Because glycans immobilized on microarrays may have different behaviors than in solution, SPR experiments were run using competition of soluble ligands with assays of BambL binding to a chip presenting multivalent fucose residues. Increasing concentrations of soluble ligands were used to determine the IC$_{50}$, as exemplified in supplemental Fig. S2. Data from inhibition assays using additional oligosaccharides are shown in Table 3, where di- and trisaccharides appear to be the

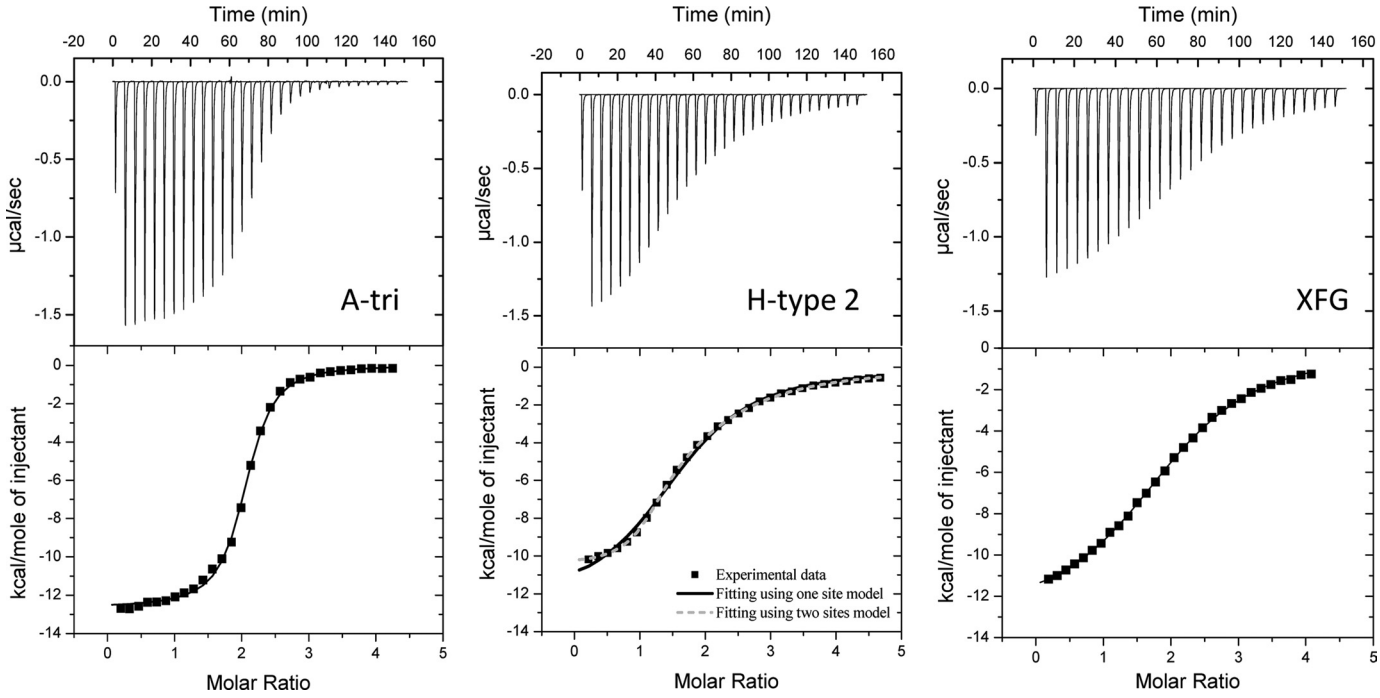

FIGURE 2. **Microcalorimetry data.** The ITC plot (measured by VP-ITC, Microcal) was obtained from the titration of BambL (22–24 μM) with several oligosaccharides (concentrations from 0.4 to 0.5 mM) at 25 °C. Protein and glycans were prepared in 20 mM Tris/HCl, pH 7.5, and 150 mM NaCl. The plots in the *lower panels* show the total heat released as a function of total ligand concentration for the titration shown in the *upper panels*. The *solid lines* represent the best least-square fit to experimental data using a one-site model. A two-site model was been used for BambL-H-type 2 interaction (*dotted lines*).

TABLE 4

Titration microcalorimetry data for the interaction between BambL and fucosylated ligands

Experiments were performed twice, and ±S.D. values are expressed for K_D and ΔH.

Ligand	Fitting model	*n*	K_D	$-\Delta G$	$-\Delta H$	$T\Delta S$
			μM	*kJ/mol*	*kJ/mol*	*kJ/mol*
A-tri	1	1.96	0.46 ± 0.02	36.0	53.1 ± 0.1	−16.9
H-type 5/FucLac	1	2.03	0.76 ± 0.07	34.9	46.3 ± 0.2	−11.3
αMeFuc	1	2.02	0.96 ± 0.03	34.3	47.8 ± 1.8	−13.5
H-di	1	2.04	1.03 ± 0.08	34.2	45.7 ± 0.2	−11.5
XFG	1	1.94	6.0 ± 0.5	29.8	53.0 ± 1.6	−23.2
H-type 2	1	1.96	7.5 ± 0.1	29.3	44.4 ± 0.7	−15.2
	2, S1	0.97	0.56 ± 0.01	35.7	47.8 ± 1.1	−12.1
	2, S2	1.10	14.0 ± 0.3	27.7	39.7 ± 0.9	−12.0
Le^Y	1	2.00	11.1 ± 0.1	28.3	38.6 ± 0.4	−10.3
Le^a	1	2[a]	18.2 ± 0.7	27.1	28.7 ± 0.1	−1.6
H-type1	1	2[a]	26.1 ± 0.1	26.2	17.6 ± 0.1	8.6
Le^X	1	1.97	34.8 ± 1.4	25.4	39.1 ± 0.2	−13.6
Le^b	1	2[a]	63.7 ± 1.2	23.9	25.4 ± 0.3	−1.5
B-penta	1	2[a]	95.3 ± 1.8	23.0	25.9 ± 1.2	−2.9
A-penta	1	2[a]	120 ± 2	22.4	13.7 ± 0.1	8.7

[a] Stoichiometry value *n* was fixed during fitting procedure.

most efficient in competing with the binding of BambL to a multivalent fucose surface, with the best inhibitors being the A-tri and H-type 5 (FucLac) trisaccharides. The Fucα1-6GlcNAc disaccharide, which was not assayed on the glycan array, appeared to be as good a ligand as other αFuc-containing disaccharides. Longer ligands had weaker inhibitory potential, consistent with the binding on the glycan array. However, H-type 2 and Le^Y performed much better than the other oligosaccharides, confirming the preference of the lectin for the Fucα1–2Galβ1–4GlcNAc motif, as demonstrated on the glycan microarray.

Determination of Affinity Constants—The binding of BambL to human glycosidic epitopes was further characterized by titration microcalorimetry to determine the association constant and thermodynamics characteristics of the interaction. Typical thermograms, such as the one obtained for A-tri, H-type 2, and XFG (Fig. 2), display strong exothermic peaks at the beginning of the titration and only residual heat at the end. Titration occurs for a molar ratio of ligand/protein around 2, indicating two binding sites/protein. Integration of data can be performed generally using a one-site binding model, although an independent two-site model yields a better fit for the H-type 2 epitope (Fig. 2). The dissociation constants listed in Table 4 indicate strong lectin-carbohydrate interactions with submicromolar values for αMeFuc, H-type 5 (FucLAc), and A-tri. The plant cell wall heptasaccharide XFG is also an excellent ligand with a dissociation constant of 6 μM. Among human histo-blood group epitopes, H-type 2 and Le^Y oligosaccharides display K_D values of 7.5 and 11.1 μM, respectively. H-type 1 trisaccharide is four times weaker than H-type 2. Blood group A is the

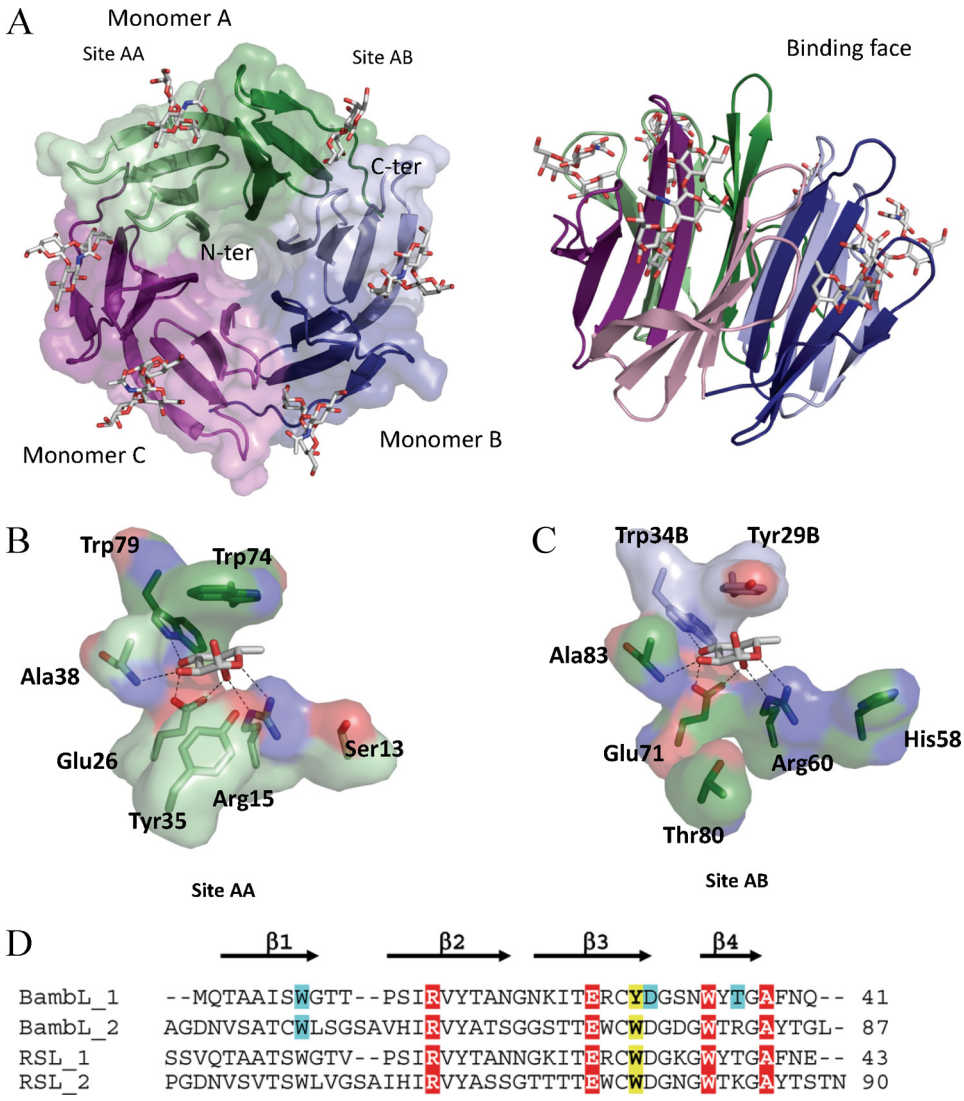

FIGURE 3. **Crystal structure of BambL/H-type 1 oligosaccharide.** *A*, two representations of the six-bladed β-propeller formed by the association of three monomers, which are colored in *green*, *blue*, and *purple*. *B* and *C*, details of the interaction between fucose and BambL lectin in the intramolecular and intermolecular binding sites, respectively. Amino acids are from chain A unless indicated otherwise. *D*, sequence alignments of the two-blade repeat of BambL and comparison with RSL. Amino acids involved in hydrogen bonds and van der Waals contact with fucose have a *red* and *yellow* background, respectively. The ones involved in hydrogen bonds with other residues of the oligosaccharides have a *blue* background.

highest affinity trisaccharide (K_D = 460 nM) but the A-type 2 pentasaccharide (A penta) is 200 times weaker. The two binding sites seem to have similar binding properties, except for the interaction with H-type 2, where the two-site model gives a better fit and indicates a high affinity site (K_D = 0.56 μM) and an affinity 25 times lower for the second site (K_D = 14 μM) (Table 4).

Analysis of the thermodynamics revealed very different contributions, depending on the ligand (Table 4). The high affinity disaccharides and trisaccharides have strong enthalpies of binding with ΔH values ranging from −44.4 to −53.1 kJ/mol, which are partially counterbalanced by unfavorable entropy contribution ($T\Delta S$ from −11.5 to −16.9). Similar behavior is observed for the high affinity oligosaccharides (XFG, H-type 2, and Le^Y). The XFG plant oligosaccharide displays the most unfavorable entropy contribution, likely because of its large number of glycosidic linkages. On the other hand, some of the low affinity ligands, such as H-type 1 trisaccharide, display very weak enthalpy of binding and favorable entropy, consistent with the poor binding of H-type 1 glycans on the microarray.

Crystal Structure of BambL and Complexes with Human Fucosylated Epitopes—Co-crystallization of BambL with different oligosaccharides gave rise to high quality crystals in about 5 days. All of the different complexed structures contain three molecules in the asymmetric unit but present different space groups and unit cells (Table 2). Because BambL presents 75% sequence identity with RSL and also exists as a trimer in solution, the RSL trimer (Protein Data Bank 2BT9) was used as a search model in the molecular replacement procedure for the FucLac complex structure. The trimer coordinates of that complex were then used to solve the other complexes structures.

All 87 amino acids of BambL could be modeled in each chain of the different structures. The N-terminal methionine was found oxidized in some case. BambL presents a six-bladed β-propeller fold generated upon trimerization where each monomer (A, B, and C) consists of two small four-

stranded anti-parallel β-sheets (Fig. 3*A*). The BambL-FucLac complex and RSL-αMeFuc structures show a root mean square deviation of 0.58 Å for 260 aligned Cα as calculated with PDBeFold (33). The BambL-FucLac complex presents very low occupancy of ligands in the binding sites with only one fucose visible between the two blades of chain C. This seems to be because of very tight packing. The structure was therefore not analyzed further.

BambL-Fucose Interaction—For the other BambL complexes obtained with B-tetra, H-type 1, and H-type 2 oligosaccharides, interaction with the ligand is visible in two sites/monomer, *i.e.* six sites/β-propeller (Fig. 3*A*). One fucose-binding site is located between the two β-sheets of a monomer (intramonomeric; Fig. 3*B*), whereas the second is at the interface between two neighboring monomers (intermonomeric; Fig. 3*C*). Although the two binding site are very similar, some differences are observed for amino acids in contact with fucose (Trp-74 in site AA *versus* Tyr-29 in site AB) or for amino acids in the vicinity (Tyr-35/Thr-80 and Ser-13/His-58). Six hydrogen bonds between the fucose and protein were observed (Fig. 3), with Arg-15, Glu-26, and Trp-79 and the main chain of Ala-38 for intramonomeric sites and Arg-60, Glu-71, and Trp-34 and the main chain of Ala-83 for the intermonomeric sites. Hydrophobic contacts also play important roles in the binding of fucose, which is the main structural difference between the intra- and intermonomeric sites. In both cases an aromatic residue stacks against the fucose hydrophobic face with a tryptophan (Trp-74) for the intramonomeric site and a tyrosine (Tyr-29) for the intermonomeric site. The features of BambL-binding sites are very close to the previously described fucose-binding site of RSL (18) (supplemental Fig. 3*S*).

BambL-B-Tetra Complex—The structure of BambL in complex with blood group B tetrasaccharide has been solved at 1.75Å (Fig. 4). The electron density map shows the α-fucose in all six sites but other monosaccharides are only visible in the intramonomeric sites with optimal electron density for the whole tetrasaccharide in sites B and C. In addition to the fucose hydrogen bond network described above, one hydrogen bond is created between O6 of the α-galactose and the main chain oxygen of Thr-36. The O2 of αGal is not close to the protein surface, rationalizing the fact that both blood group B (αGal) and blood group A (αGalNAc) bind with the same affinity.

When considering the narrow funnel-shaped binding site (Fig. 4), the tetrasaccharide appears to be in a rather constrained conformation. Indeed, when analyzing the torsion angles at each glycosidic linkage (Fig. 5 and supplemental Table S3), the Galα1–3Gal linkage is characterized by Φ and Ψ angles close to 140° for each. From previously calculated energy maps of this linkage (34), this conformation is about 4 kcal above the global minimum at (80° and 90°) (Fig. 5). The steric hindrance around the central galactose explains this constrained conformation. The situation would be different with a less branched trisaccharide explaining the much higher affinity of A-tri compared with a longer oligosaccharide with substituted galactose.

BambL-H-type 1 Tetrasaccharide Complex—The structure of BambL complexed with H-type 1 tetrasaccharide has been solved at 1.6 Å resolution. As described above, all binding sites are occupied, but only site C displays the whole tetrasaccharide. In addition to the main fucose-binding network, two hydrogen bonds are created between the *N*-acetyl oxygen and the O4 of GlcNAc and between the side chains of Trp-74 and Asp-30, respectively (Fig. 4). Another hydrogen bond is observed between the O4 of the reducing Gal and the nitrogen side chain of Trp-8. Three water molecules are involved in bridging interactions between the oligosaccharide in the protein. As observed for the BambL-B-tetra complex, the Gal residue linked to the Fuc is not involved in direct interactions. Analysis of the conformations at the glycosidic linkages indicates that the Fucα1–2Gal linkage adopts a low energy conformation, but the Galβ1–3GlcNAc linkage is distorted with μ angle values ranging between −37 and −56° (Fig. 5 and supplemental Table S3) and an energy cost of 3 to 5 kcal/mol.

BambL-H-type 2 Tetrasaccharide Complex—In the BambL-H-type 2 tetrasaccharide complex (1.68 Å resolution), clear electronic density for trisaccharides is observed in five of the six binding sites, and only Fuc can be observed in site BC. Although fucose is always bound in the same way in the main binding sites, the interactions with oligosaccharides are different for the intermolecular site and the intramolecular ones (Fig. 4). In the intramolecular sites (A, B, and C), two water-mediated hydrogen bonds are established between the O6 and nitrogen of GlcNAc and the Trp-74 and Asp-30 side chains, respectively. In the intermolecular sites (AB and CA), the GlcNAc residue is oriented in a different manner, and a direct hydrogen bond is observed between the oxygen of the *N*-acetyl group and Trp-51 and a second one between O4 and the side chain of Arg-60. These different orientations of the GlcNAc residue are due to very different conformations of the βGal1–4GlNac linkage (supplemental Table S3). In the intramonomeric sites, Φ and Ψ torsion angles close to −70° and −130° are observed, corresponding to the energy minimum (Fig. 5). Conversely, in the intermonomeric binding sites, conformations with Φ and Ψ close to −70° and 80° are observed, corresponding to a 150° tilt in the Ψ angle as compared with the previous one. This particular conformation corresponds to a secondary minimum on the energy maps with energy about 3 kcal/mol greater than the minimum (Fig. 5). This energy difference is easily compensated by the two direct hydrogen bonds that are observed between the GlcNAc residue and the protein in these sites.

The observation of two types of sites is in agreement with the ITC data. Only for H-type 2 tetrasaccharide, a two site model was required to fit with the experimental data. The two sites are slightly different in amino acid composition around the GlcNAc residues, with Ser-13 and Trp-74 in intramolecular site correspond to His-58 and Tyr-29 in the intermolecular one. As described above, the two sites differ by the number of hydrogen bonds to GlcNAc and by the conformational constraints. Nevertheless, the structural information does not allow for the identification of the medium affinity binding site ($K_D = 14\ \mu M$) and the high affinity binding site ($K_D = 0.56\ \mu M$) determined by ITC.

Binding of BambL to Giant Unilamellar Vesicles—As a next step, the binding of BambL to human glycosidic epitopes was tested in a membranous environment by using GUVs that contained glycosphingolipids. The GUVs (typical diameter, 10–30

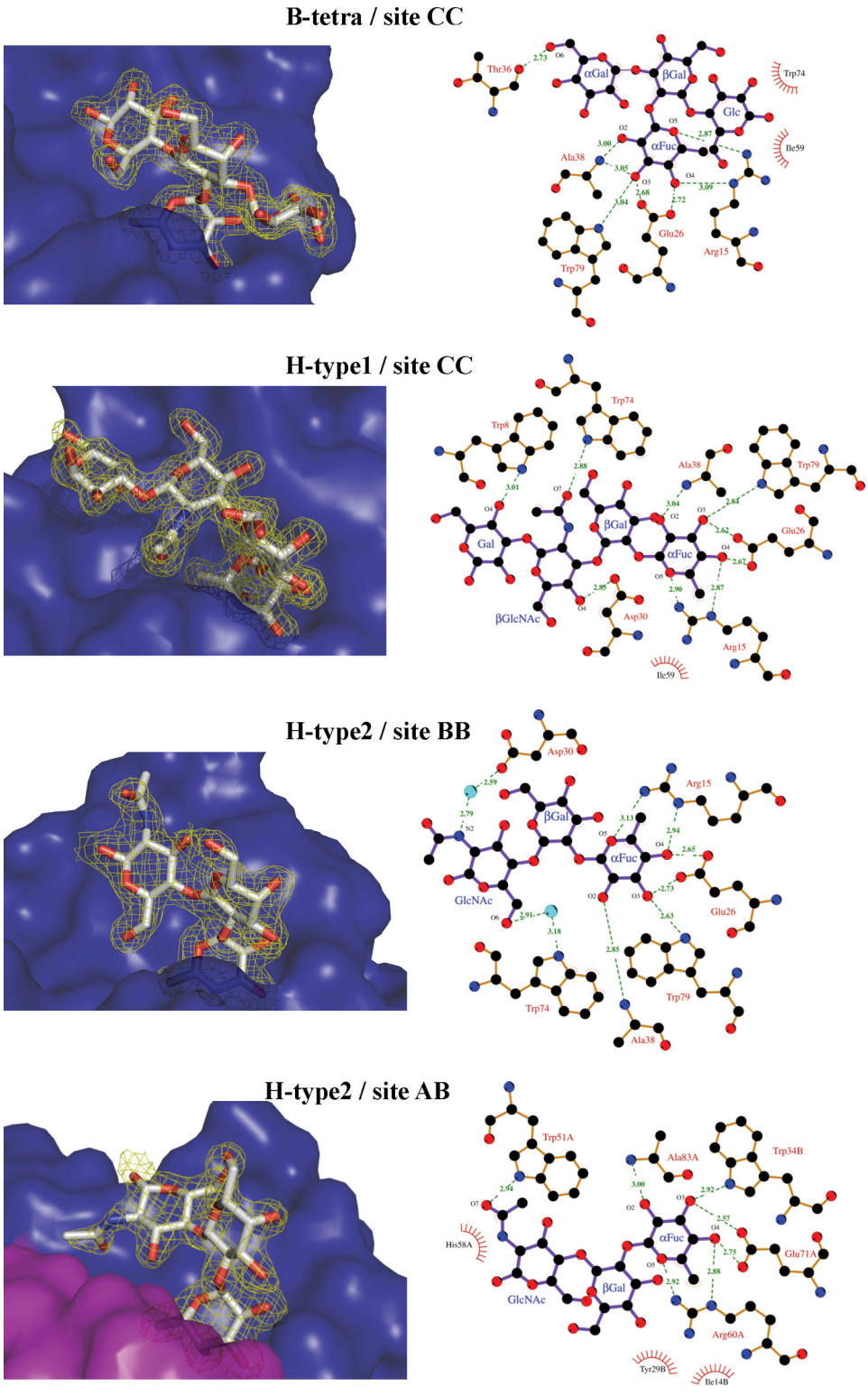

FIGURE 4. **Binding of fucosylated oligosaccharides by BambL.** $2mF_o - DF_c$ electron density maps contoured at 1σ are represented in the *left-hand panels*. The solvent-accessible surface of the protein is shown in *blue* for one monomer and *magenta* for the other. Interactions between BambL and oligosaccharides are represented in the *right-hand panels* with details of hydrogen bond distances. Two-dimensional plots, created using LIGPLOT, display all of the amino acids interacting with oligosaccharides and bridging water molecules with details of hydrogen bond distances.

μm) composed of DOPC (64 mol %; spiked with 1 mol % BODIPY-FL-C5-HPC, green), cholesterol (30 mol %), and various glycosphingolipids (5 mol %) were observed by fluorescence microscopy on incubation with Cy3-labeled BambL at room temperature (supplemental Fig. S4).

Our experiments on GUVs clearly indicated that fucose is an absolute requirement for the binding of BambL. BambL does not bind to liposomes (composed only of the phospholipid DOPC (data not shown)), lactotetraosylceramide (the non-fucosylated precursor of ABO and Lewis blood group

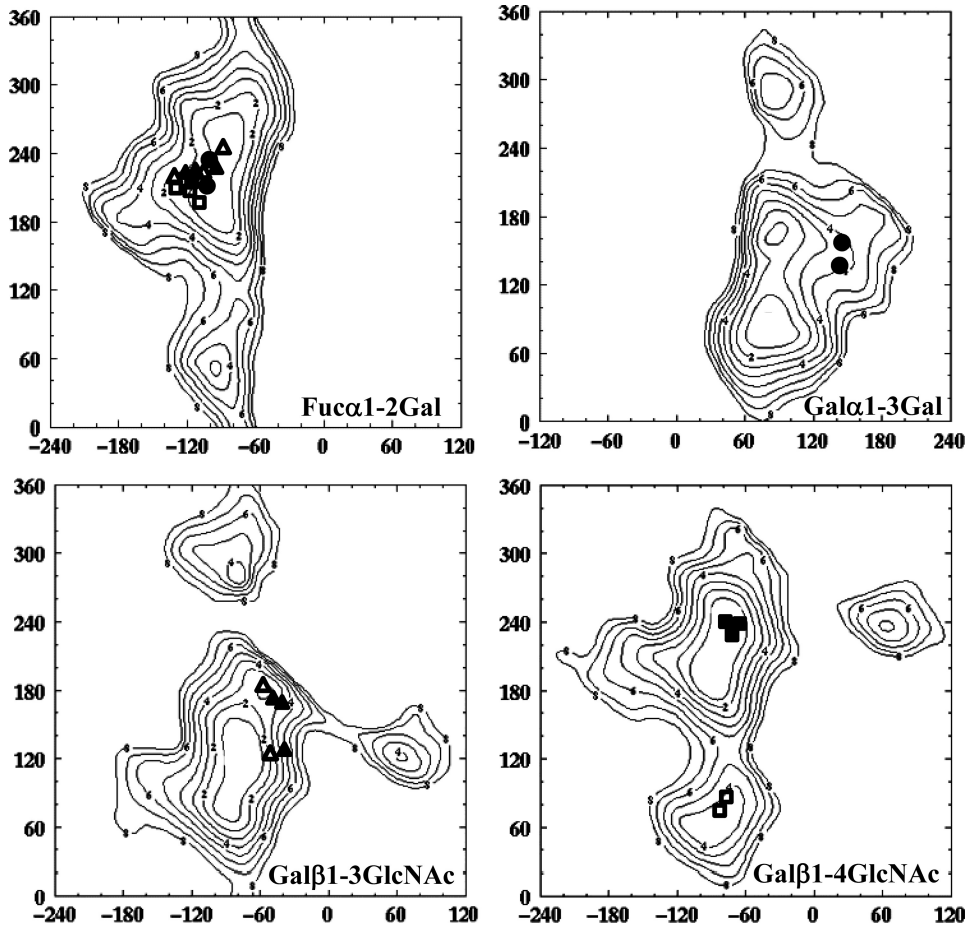

FIGURE 5. **Conformations of glycosidic linkages of bound oligosaccharides reported on the corresponding MM3 energy maps available at the Glyco3D site.** H-type 1 oligosaccharide conformations are represented by *triangles*, H-type 2 by *squares*, and B-tetra by *circles*. *Filled* and *open symbols* are for oligosaccharides in the intra- and intermolecular sites, respectively.

antigens), or globotriaosylceramide (which belongs to the globoseries).

BambL bound to almost all of the Lewis type 1, and ABO blood group glycosphingolipids, with a clear preference for blood groups H and Lewis a. Binding to Lewis b and blood groups A and B antigens was significantly reduced, most likely because of the additional sugar in the binding cavity. For "ALewis b," *i.e.* Lewis b oligosaccharide with a terminal nonreducing αGalNAc residue, the most complex glycosphingolipid used in the type 1 series, hardly any binding of BambL was detected, probably because of the two additional sugars. We were not able to see a superior binding of BambL to glycosphingolipids of the type 2 series represented by Lewis X and Lewis Y compared with their isoforms in the type 1 series, Lewis a and Lewis b. One reason might be differences in the fatty acid composition of the receptor glycosphingolipid, which seems to be important for the binding of lectins (35). All glycosphingolipids of the type 1 series were isolated from human meconium, and the type 2 species were isolated from dog intestines (28). The less prominent differences in binding avidity of BambL to type 1 and type 2 glycosphingolipid species might result from lectin-induced glycosphingolipid clustering in a highly dynamic membrane environment.

Binding to Human Saliva and Tissues—To get a better insight into the specificity of BambL and to evaluate the impact of the combined *ABO*, *FUT2*, and *FUT3* polymorphisms on the ability of BambL to recognize human histo-blood group diversity, its binding to saliva samples was determined through an enzyme-linked lectin assay (Fig. 6*A*). The difference from the fucose-specific plant lectin UEA-I used as a positive control is shown on Fig. 6*B*; the specificity of BambL binding to either secretor or nonsecretor saliva samples was ascertained through its complete inhibition by either fucose or 2′-fucosyllactose (Fig. 6*C*). BambL was able to recognize all saliva samples, including nonsecretor saliva ($FUT2^{-/-}$) and Lewis negative saliva ($FUT3^{-/-}$). Nevertheless, despite individual variations within subgroups, a significantly weaker binding was observed on saliva from nonsecretor individuals compared with secretor individuals, consistent with the IC_{50} results determined by SPR and the affinity measurements. Likewise, the presence of the A or B epitopes decreased saliva recognition since the lectin binding to O-type secretors was stronger than to non-O-type secretor saliva. Among secretors, no effect of the Lewis phenotype was observed. However, a significantly weaker binding was observed on the saliva of nonsecretor Lewis negative individuals. Thus a combination of the lack of both FUT2 (secretor) and FUT3 (Lewis) enzyme activities, together with the presence of the A or B epitopes, reduces BambL binding to human saliva mucins. The specificity of BambL differs from

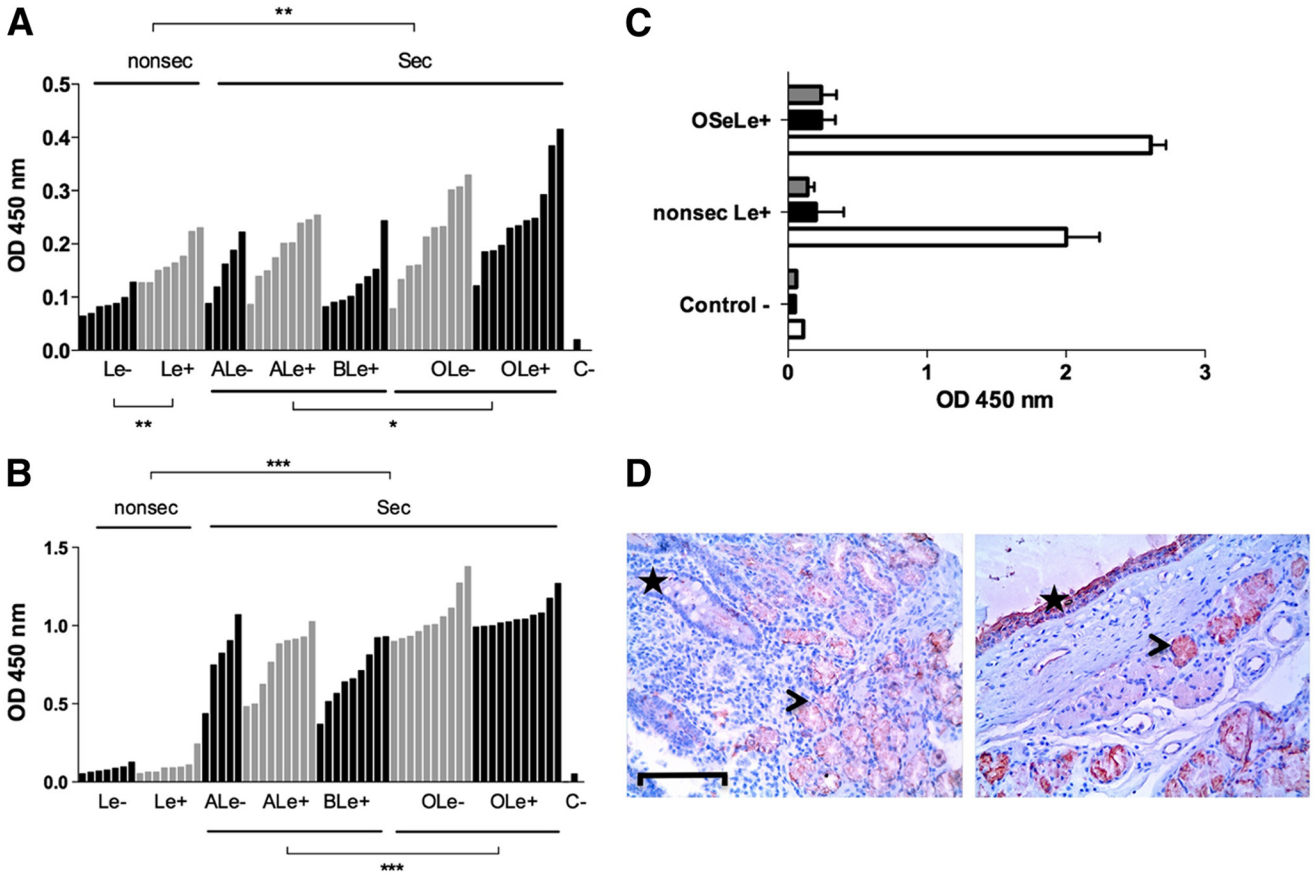

FIGURE 6. **Binding of labeled BambL and UEA-I to human saliva and tissues.** *A*, saliva samples were collected from 59 healthy individuals of known ABO, secretor, and Lewis phenotypes. Each *bar* represents binding of BambL at 0.1 μg/ml to an individual saliva sample as the mean OD values of duplicates. Samples are grouped by their histo-blood type and ranked by OD values within each subgroup. The negative control value in the absence of saliva (BSA only) is depicted by *C*−. Comparisons between subgroups were performed using a two-tailed Mann-Whitney test (*, $p < 0.02$; **, $p < 0.01$). *B*, binding of UEA-I at 1 μg/ml to individual saliva samples as presented above. Comparisons between subgroups were performed using a two-tailed Mann-Whitney test (***, $p < 0.0001$). *C*, inhibition of BambL binding to saliva from either O secretor Lewis positive (*OSeLe*+) or nonsecretor Lewis positive (*nonsec Le*+) saliva samples by 100 mM fucose (*black bars*) or 5 mM 2′-fucosyllactose (*gray bars*). OD values in the absence of inhibitor are shown with *white bars*. Values represent mean values ± S.D. of two samples in duplicate. *Control* − denotes negative control value in the absence of saliva. *D*, staining by biotinylated BambL of tissue sections from the duodenum of a nonsecretor Lewis positive individual (*left*) and the trachea from an O secretor Lewis positive donor (*right*). *Bar* = 100 μm. The specific staining appears in *red* and hematoxylin counterstaining in *blue*. On the *left panel*, the location of the crypts of Lieberkühn with unstained goblet cells is shown by a *star*, and the location of the stained Brünner glands is shown by an *arrowhead*. On the *right panel*, the surface epithelium of the trachea is shown by a *star*, and the *arrowhead* indicates the location of a stain-associated mucous gland.

that of UEA-I, which hardly recognized nonsecretor saliva samples, although, quite similar to BambL, it showed a significantly lower binding to saliva from non-O-type individuals among secretors. Yet, at variance with BambL, no effect of the Lewis phenotype was visible among either secretors or nonsecretors.

To gain insight into the localization of BambL-binding epitopes in human tissues, a histochemical analysis was performed. Binding for the most part was restricted to epithelial cells, although some weak staining could be observed on the vascular endothelium (Fig. 6*D*). No clear impact of the ABO secretor or Lewis status of the tissue donor could be observed; however, no tissue sample from a nonsecretor Lewis negative individual was available to assay. In the respiratory tract, in addition to a clear staining of the bronchial epithelial cells, the strongest staining was observed on the mucous-producing glands lining the trachea and bronchi. In the gastroduodenal junction, labeling of the surface epithelia of both the pyloric and duodenal regions was seen in all individuals tested, albeit at a lower intensity in nonsecretors, along with a strong staining of the pyloric glands and the Brünner glands of the duodenum.

DISCUSSION

Fucose-binding proteins with β-propeller folds belong to a recently described lectin family (18, 36). This group is characterized by a strong affinity for fucose and a high valency, with six binding sites in proper orientation for binding to glycoconjugates on membranes. BambL is the first lectin of this family to have been identified in a human pathogen genome, and our present work highlights its preference for blood group H and Lewis Y oligosaccharides resulting in stronger binding to humans with both O and secretor phenotypes. Binding to the Lewis a epitope was accounted for by the stronger binding to Lewis positive phenotype individuals in the absence of blood group H or Lewis Y (nonsecretors).

The analyses to determine the specificity of BambL, as reported here, were quite extensive and involved the identification of candidate glycans using the Consortium for Functional Glycomics glycan microarray to subsequently select a

panel of glycan structures for a more detailed analysis using physical methods including SPR, ITC, and binding to glycolipids in giant unilammelar vesicles. Interestingly, the data for the relative binding of BambL to the glycans on the microarray were in very close agreement with the observations made using the solution equilibrium method of ITC as well as the equilibrium method of SPR and unilamellar binding method with fucosylated glycosphingolipids. Thus, the screening of hundreds of glycans on a microarray provides a rapid, high throughput approach that approximates the more time-consuming and labor-intensive physical methods and allows a quick screen to select glycans for more rigorous and quantitative physical methods of analysis.

Recent evidence strongly suggests that the relationship between histo-blood group phenotypes and susceptibility to infection is a result of co-evolution between mammals and pathogens (37–39). Polymorphism in the fucosyltransferase genes is responsible for a large part of the variability of glycan structures present on human epithelia. The *FUT2* "secretor" gene encodes the fucosyltransferase that synthesizes the H antigen, and its loss of activity results in the absence of ABH antigens in the lung, saliva, and gut, *i.e.* the "nonsecretor" phenotype. In parallel, the loss of function of the *FUT3* "Lewis" gene results in the Lewis negative phenotype (40).

At the present time, only a limited number of pathogen receptors have been demonstrated to be responsible for the binding to specific blood group oligosaccharides. Most of them are from enteropathogenic microbes such as *Helicobacter pylori* (41), *Vibrio cholerae* (42), or noroviruses (43). As for lung pathogens involved in life-threatening infections in cystic fibrosis patients, two lectins specific for galactose and fucose have been characterized (44, 45). However, a recent clinical study performed on a group of CF patients did not find any association between the ABO blood group, secretor, and Lewis phenotype and the severity of *P. aeruginosa* infections (46). No such study has been performed yet on bacteria of the *Burkholderia* complex, but as glycoconjugates fucosylation is increased in the lung tissue of CF patients (47), histo-blood group oligosaccharides are a promising target for *Burkholderia* lectins.

Opportunistic bacteria in the environment of CF patients are at the origin of lung infections. *P. aeruginosa* and Bcc bacteria are environmental bacteria able to colonize a large variety of niches. *B. ambifaria* is more particularly associated with the plant rhizosphere. Fucose appears to be a common epitope between plant and mammals. It is part of the hemicellulose fraction of the plant cell wall and is present on plant *N*-glycoproteins (48). Our results demonstrate that BambL binds efficiently to both plant and human fucosylated oligosaccharides. If BambL is expressed and present on the bacterial surface, that remains to be demonstrated, and the lectin may therefore be involved in the easy niche adaptation observed for *B. ambifaria*.

The present work has deciphered the molecular basis of the specificity of BambL toward fucosylated oligosaccharides. It has thus contributed to the current efforts to understand the glyco-strategies of human opportunistic pathogens and to develop glyco-based compounds with anti-adhesive properties against such pathogens.

Acknowledgments—The glycan array resources were provided by the Consortium for Functional Glycomics (GM62116). Crystal data collection was performed at the European Synchrotron Radiation Facility, and we are grateful for the assistance in using beamline BM30A. Access to the High Throughput Crystallization facility of the Partnership for Structural Biology (PSB) in Grenoble was supported by the European Community PCube program.We acknowledge the help received from the Cell and Tissue Imaging Core Facility of the Institut Curie (PICT-IBiSA) and the staff of the Life Imaging Center (LIC) Freiburg and the use of the advanced microscopy equipment of the LIC Freiburg and the Nikon Imaging Center at the Institut Curie-CNRS. We also thank the MicroPiCell core facility of IFR26, Nantes, for the preparation of tissue microarrays.

REFERENCES

1. Vanlaere, E., Baldwin, A., Gevers, D., Henry, D., De Brandt, E., LiPuma, J. J., Mahenthiralingam, E., Speert, D. P., Dowson, C., and Vandamme, P. (2009) Taxon K, a complex within the *Burkholderia cepacia* complex, comprises at least two novel species, *Burkholderia contaminans* sp. nov. and *Burkholderia lata* sp. nov. *Int. J. Syst. Evol. Microbiol.* **59,** 102–111
2. Vanlaere, E., Lipuma, J. J., Baldwin, A., Henry, D., De Brandt, E., Mahenthiralingam, E., Speert, D., Dowson, C., and Vandamme, P. (2008) *Burkholderia latens* sp. nov., *Burkholderia diffusa* sp. nov., *Burkholderia arboris* sp. nov., *Burkholderia seminalis* sp. nov., and *Burkholderia metallica* sp. nov., novel species within the *Burkholderia cepacia* complex. *Int. J. Syst. Evol. Microbiol.* **58,** 1580–1590
3. Schmidt, S., Blom, J. F., Pernthaler, J., Berg, G., Baldwin, A., Mahenthiralingam, E., and Eberl, L. (2009) Production of the antifungal compound pyrrolnitrin is quorum sensing-regulated in members of the *Burkholderia cepacia* complex. *Environ. Microbiol.* **11,** 1422–1437
4. Chiarini, L., Bevivino, A., Dalmastri, C., Tabacchioni, S., and Visca, P. (2006) *Burkholderia cepacia* complex species: health hazards and biotechnological potential. *Trends Microbiol.* **14,** 277–286
5. Saiman, L., and Siegel, J. (2004) Infection control in cystic fibrosis. *Clin. Microbiol. Rev.* **17,** 57–71
6. Valvano, M. A., Keith, K. E., and Cardona, S. T. (2005) Survival and persistence of opportunistic *Burkholderia* species in host cells. *Curr. Opin. Microbiol.* **8,** 99–105
7. Aaron, S. D., Ferris, W., Henry, D. A., Speert, D. P., and Macdonald, N. E. (2000) Multiple combination bactericidal antibiotic testing for patients with cystic fibrosis infected with *Burkholderia cepacia*. *Am. J. Respir. Crit. Care Med.* **161,** 1206–1212
8. Coenye, T., Mahenthiralingam, E., Henry, D., LiPuma, J. J., Laevens, S., Gillis, M., Speert, D. P., and Vandamme, P. (2001) *Burkholderia ambifaria* sp. nov., a novel member of the *Burkholderia cepacia* complex including biocontrol and cystic fibrosis-related isolates. *Int. J. Syst. Evol. Microbiol.* **51,** 1481–1490
9. Pirone, L., Chiarini, L., Dalmastri, C., Bevivino, A., and Tabacchioni, S. (2005) Detection of cultured and uncultured *Burkholderia cepacia* complex bacteria naturally occurring in the maize rhizosphere. *Environ. Microbiol.* **7,** 1734–1742
10. Parke, J. L., and Gurian-Sherman, D. (2001) Diversity of the *Burkholderia cepacia* complex and implications for risk assessment of biological control. *Annu. Rev. Phytopath.* **39,** 225–258
11. Vial, L., Lépine, F., Milot, S., Groleau, M. C., Dekimpe, V., Woods, D. E., and Déziel, E. (2008) *Burkholderia pseudomallei*, *B. thailandensis*, and *B. ambifaria* produce 4-hydroxy-2-alkylquinoline analogues with a methyl group at the 3 position that is required for quorum-sensing regulation. *J. Bacteriol.* **190,** 5339–5352
12. Imberty, A., and Varrot, A. (2008) Microbial recognition of human cell surface glycoconjugates. *Curr. Opin. Struct. Biol.* **18,** 567–576
13. Pieters, R. J. (2011) Carbohydrate-mediated bacterial adhesion. *Adv. Exp.*

Med. Biol. **715,** 227–240
14. Glick, M. C., Kothari, V. A., Liu, A., Stoykova, L. I., and Scanlin, T. F. (2001) Activity of fucosyltransferases and altered glycosylation in cystic fibrosis airway epithelial cells. *Biochimie* **83,** 743–747
15. Mitchell, E., Houles, C., Sudakevitz, D., Wimmerova, M., Gautier, C., Pérez, S., Wu, A. M., Gilboa-Garber, N., and Imberty, A. (2002) Structural basis for oligosaccharide-mediated adhesion of *Pseudomonas aeruginosa* in the lungs of cystic fibrosis patients. *Nat. Struct. Biol.* **9,** 918–921
16. Sulák, O., Cioci, G., Delia, M., Lahmann, M., Varrot, A., Imberty, A., and Wimmerová, M. (2010) A TNF-like trimeric lectin domain from *Burkholderia cenocepacia* with specificity for fucosylated human histo-blood group antigens. *Structure* **18,** 59–72
17. Sulák, O., Cioci, G., Lameignère, E., Balloy, V., Round, A., Gutsche, I., Malinovská, L., Chignard, M., Kosma, P., Aubert, D. F., Marolda, C. L., Valvano, M. A., Wimmerová, M., and Imberty, A. (2011) *Burkholderia cenocepacia* BC2L-C is a super lectin with dual specificity and proinflammatory activity. *PLoS Pathog.* **7,** e1002238
18. Kostlánová, N., Mitchell, E. P., Lortat-Jacob, H., Oscarson, S., Lahmann, M., Gilboa-Garber, N., Chambat, G., Wimmerová, M., and Imberty, A. (2005) The fucose-binding lectin from *Ralstonia solanacearum*. A new type of beta-propeller architecture formed by oligomerization and interacting with fucoside, fucosyllactose, and plant xyloglucan. *J. Biol. Chem.* **280,** 27839–27849
19. Smith, D. F., Song, X., and Cummings, R. D. (2010) Use of glycan microarrays to explore specificity of glycan-binding proteins. *Methods Enzymol.* **480,** 417–444
20. Leslie, A. G. W., and Powell, H. R. (2007) Processing diffraction data with mosflm, *NATO Science Series* **245,** 41–51
21. Collaborative Computational Project, Number 4 (1994) The CCP4 suite: programs for protein crystallography. *Acta Crystallogr. D Biol. Crystallogr.* **50,** 760–763
22. McCoy, A. J., Grosse-Kunstleve, R. W., Adams, P. D., Winn, M. D., Storoni, L. C., and Read, R. J. (2007) Phaser crystallographic software. *J. Appl. Crystallogr.* **40,** 658–674
23. Brünger, A. T. (1992) Free R-value – a novel statistical quantity for assessing the accuracy of crystal-structures. *Nature* **355,** 472–475
24. Murshudov, G. N., Vagin, A. A., and Dodson, E. J. (1997) Refinement of macromolecular structures by the maximum likelihood method. *Acta Crystallogr. D Biol. Crystallogr.* **53,** 240–255
25. Emsley, P., Lohkamp, B., Scott, W. G., and Cowtan, K. (2010) Features and development of Coot. *Acta Crystallogr. D Biol. Crystallogr.* **66,** 486–501
26. Laskowski, R. A., Macarthur, M. W., Moss, D. S., and Thornton, J. M. (1993) *J. Appl. Crystallogr.* **26,** 283–291
27. Wallace, A. C., Laskowski, R. A., and Thornton, J. M. (1995) LIGPLOT: a program to generate schematic diagrams of protein-ligand interactions. *Protein Eng.* **8,** 127–134
28. Karlsson, K. A., and Larson, G. (1981) Molecular characterization of cell surface antigens of fetal tissue. Detailed analysis of glycosphingolipids of meconium of a human O Le(a−b+) secretor. *J. Biol. Chem.* **256,** 3512–3524
29. Mathivet, L., Cribier, S., and Devaux, P. F. (1996) Shape change and physical properties of giant phospholipid vesicles prepared in the presence of an AC electric field. *Biophys. J.* **70,** 1112–1121
30. Römer, W., Berland, L., Chambon, V., Gaus, K., Windschiegl, B., Tenza, D., Aly, M. R., Fraisier, V., Florent, J. C., Perrais, D., Lamaze, C., Raposo, G., Steinem, C., Sens, P., Bassereau, P., and Johannes, L. (2007) Shiga toxin induces tubular membrane invaginations for its uptake into cells. *Nature* **450,** 670–675
31. Azevedo, M., Eriksson, S., Mendes, N., Serpa, J., Figueiredo, C., Resende, L. P., Ruvoën-Clouet, N., Haas, R., Borén, T., Le Pendu, J., and David, L. (2008) Infection by *Helicobacter pylori* expressing the BabA adhesin is influenced by the secretor phenotype. *J. Pathol.* **215,** 308–316
32. Marionneau, S., Airaud, F., Bovin, N. V., Le Pendu, J., and Ruvoen-Clouet, N. (2005) Influence of the combined ABO, FUT2, and FUT3 polymorphism on susceptibility to Norwalk virus attachment. *J. Infect. Dis.* **192,** 1071–1077
33. Krissinel, E., and Henrick, K. (2004) Secondary structure matching (SSM), a new tool for fast protein structure alignment in three dimensions. *Acta Crystallogr. D Biol. Crystallogr.* **60,** 2256–2268
34. Imberty, A., Mikros, E., Koca, J., Mollicone, R., Oriol, R., and Pérez, S. (1995) Computer simulation of histo-blood group oligosaccharides: energy maps of all constituting disaccharides and potential energy surfaces of 14 ABH and Lewis carbohydrate antigens. *Glycoconj. J.* **12,** 331–349
35. Kiarash, A., Boyd, B., and Lingwood, C. A. (1994) Glycosphingolipid receptor function is modified by fatty acid content. Verotoxin 1 and verotoxin 2c preferentially recognize different globotriaosyl ceramide fatty acid homologues. *J. Biol. Chem.* **269,** 11138–11146
36. Wimmerova, M., Mitchell, E., Sanchez, J. F., Gautier, C., and Imberty, A. (2003) Crystal structure of fungal lectin. Six-bladed beta-propeller fold and novel fucose recognition mode for *Aleuria aurantia* lectin. *J. Biol. Chem.* **278,** 27059–27067
37. Aspholm-Hurtig, M., Dailide, G., Lahmann, M., Kalia, A., Ilver, D., Roche, N., Vikström, S., Sjöström, R., Lindén, S., Bäckström, A., Lundberg, C., Arnqvist, A., Mahdavi, J., Nilsson, U. J., Velapatiño, B., Gilman, R. H., Gerhard, M., Alarcon, T., López-Brea, M., Nakazawa, T., Fox, J. G., Correa, P., Dominguez-Bello, M. G., Perez-Perez, G. I., Blaser, M. J., Normark, S., Carlstedt, I., Oscarson, S., Teneberg, S., Berg, D. E., and Borén, T. (2004) Functional adaptation of BabA, the *H. pylori* ABO blood group antigen binding adhesin. *Science* **305,** 519–522
38. Ferrer-Admetlla, A., Sikora, M., Laayouni, H., Esteve, A., Roubinet, F., Blancher, A., Calafell, F., Bertranpetit, J., and Casals, F. (2009) A natural history of FUT2 polymorphism in humans. *Mol. Biol. Evol.* **26,** 1993–2003
39. Nyström, K., Le Gall-Reculé, G., Grassi, P., Abrantes, J., Ruvoën-Clouet, N., Le Moullac-Vaidye, B., Lopes, A. M., Esteves, P. J., Strive, T., Marchandeau, S., Dell, A., Haslam, S. M., and Le Pendu, J. (2011) Histo-blood group antigens act as attachment factors of rabbit hemorrhagic disease virus infection in a virus strain-dependent manner. *PLoS Pathog.* **7,** e1002188
40. Marionneau, S., Cailleau-Thomas, A., Rocher, J., Le Moullac-Vaidye, B., Ruvoën, N., Clément, M., and Le Pendu, J. (2001) ABH and Lewis histo-blood group antigens, a model for the meaning of oligosaccharide diversity in the face of a changing world. *Biochimie* **83,** 565–573
41. Lindén, S., Mahdavi, J., Semino-Mora, C., Olsen, C., Carlstedt, I., Borén, T., and Dubois, A. (2008) Role of ABO secretor status in mucosal innate immunity and *H. pylori* infection. *PLoS Pathog.* **4,** e2
42. Holmner, A., Mackenzie, A., and Krengel, U. (2010) Molecular basis of cholera blood group dependence and implications for a world characterized by climate change. *FEBS Lett.* **584,** 2548–2555
43. Le Pendu, J., Ruvoën-Clouet, N., Kindberg, E., and Svensson, L. (2006) Mendelian resistance to human norovirus infections. *Semin. Immunol.* **18,** 375–386
44. Gilboa-Garber, N. (1982) Pseudomonas aeruginosa lectins. *Methods Enzymol.* **83,** 378–385
45. Imberty, A., Wimmerová, M., Mitchell, E. P., and Gilboa-Garber, N. (2004) Structures of the lectins from *Pseudomonas aeruginosa*: insight into the molecular basis for host glycan recognition. *Microbes Infect.* **6,** 221–228
46. Taylor-Cousar, J. L., Zariwala, M. A., Burch, L. H., Pace, R. G., Drumm, M. L., Calloway, H., Fan, H., Weston, B. W., Wright, F. A., and Knowles, M. R. (2009) Histo-blood group gene polymorphisms as potential genetic modifiers of infection and cystic fibrosis lung disease severity. *PLoS One* **4,** e4270
47. Scanlin, T. F., and Glick, M. C. (2001) Glycosylation and the cystic fibrosis transmembrane conductance regulator. *Respir. Res.* **2,** 276–279
48. Staudacher, E., Altmann, F., Wilson, I. B., and März, L. (1999) Fucose in *N*-glycans: from plant to man. *Biochim. Biophys. Acta* **1473,** 216–236